American Mineralogist, Volume 83, pages 1277–1284, 1998

Cation dynamics and premelting in lithium metasilicate (Li_2SiO_3) and sodium metasilicate (Na_2SiO_3): A high-temperature NMR study

Anna M. George,[1] Pascal Richet,[1,]* and Jonathan F. Stebbins[1,]†

[1]Department of Geological and Environmental Sciences, Stanford University, Stanford, California 94305-2115 U.S.A.

Abstract

Premelting effects are common in silicates and have been mostly observed as significant heat capacity anomalies beginning 100 to 200 °C below congruent melting points. To assess the role of cation dynamics in this phenomenon, we collected nuclear magnetic resonance (NMR) spectra and relaxation time data to within 20 to 50 °C of the melting points of sodium metasilicate (Na_2SiO_3), which displays a large premelting effect, and isostructural lithium metasilicate (Li_2SiO_3), which displays little premelting. From ^{7}Li NMR, Li^+ site hopping is clearly observed in Li_2SiO_3 by a partial averaging of the ^{7}Li quadrupolar peak shape, requiring exchange among a few, ordered orientations of LiO_4 tetrahedra. From ^{23}Na NMR, Na^+ site hopping in Na_2SiO_3 appears to involve a more liquid-like behavior, implying exchange among many sites with different orientations in a disordered fashion. For this phase, ^{29}Si spectra indicate that in an oxidizing environment, no liquid phase is present at 20 °C below the melting point, well within the calorimetric premelting regime. However, partial averaging of the low-temperature, biaxial chemical shift powder pattern (typical of Si sites in chain silicates) occurs, suggesting some kind of extensive, librational motion of SiO_4 tetrahedra that is possibly linked to rapid Na^+ diffusion near the melting point. In contrast to the simple Li^+ diffusion in Li_2SiO_3, this process may require considerable non-vibrational energy and may thus be related to the heat capacity anomaly just prior to melting.

Introduction

As observed for other classes of crystals (Ubbelohde 1978), crystalline silicates often undergo non-quenchable configurational changes when the melting point is approached. These changes are most simply revealed by anomalous increases in heat capacity that begin as much as 100 to 200° below the congruent melting point and account for up to 20% of the reported enthalpies of fusion (Richet and Fiquet 1991; Richet et al. 1994). Such premelting effects could have practical implications for thermodynamic analyses of high-temperature phase equilibria, but their scientific interest lies mainly in that they reveal dynamical processes in the crystalline state, which may in part resemble those that take place in melts. However, the microscopic mechanisms of such premelting effects are still only poorly known.

Comparisons between lithium (Li_2SiO_3) and sodium (Na_2SiO_3) metasilicates are especially informative (Richet et al. 1996). Both crystals have orthorhombic symmetry at room temperature (space group $Cmc2_1$) and are made up of chains of SiO_4 tetrahedra along the *c* axis linked by either NaO_5 trigonal bipyramids (McDonald and Cruickshank 1967) or by LiO_4 tetrahedra (Hesse 1977; Völlenkle 1981). Although isostructural at room temperature, these crystals behave differently when heated. Up to its melting point at 1201 °C, Li_2SiO_3 expands smoothly, shows minor changes in Raman spectra (Richet et al. 1996), and displays almost no calorimetric premelting (Stebbins et al. 1984; Téqui et al. 1992). In contrast, Na_2SiO_3 first undergoes a transition at about 577 °C from orthorhombic $Cmc2_1$ symmetry to a lower symmetry [possibly $Pmc2_1$ (Richet et al. 1996)] and then exhibits a wide premelting range of 160 °C (Naylor 1945; Richet et al. 1984) before it melts congruently at 1089 °C (Kracek 1930). The onset of premelting near 930 °C corresponds to temperatures at which extensive deformation of the silicate chains was hypothesized from similarities in the Raman spectra of the crystalline and liquid phases. In addition, some changes in the low-frequency part of the Raman spectra were interpreted as indicating the onset of high alkali mobility several hundred degrees below the melting point in both compounds (Richet et al. 1996).

Nuclear magnetic resonance (NMR) is well suited to complement the description of the structural and physical properties of these compounds at high temperatures because it gives information not only on the local environment of a given element, but also on its dynamics. Nuclear magnetic resonance has already proven to be a

* Permanent address: Laboratoire des Géomatériaux, Institute de Physique du Globe; 4, place Jussieu; 75252 Paris cedex 05; France.

† E-mail: stebbins@pangea.stanford.edu

0003–004X/98/1112–1277$05.00

useful tool to investigate the progressive change from solid- to liquid-like behavior at the glass transition (Farnan and Stebbins 1994; Stebbins 1995a) and was extensively used to characterize the dynamics of displacive phase changes and ionic conduction in crystalline solids (Rigamonti 1984; Stebbins et al. 1989; Spearing et al. 1992; Phillips et al. 1993; Spearing et al. 1994; Stebbins et al. 1995; Xu and Stebbins 1995b). Because of the relatively low melting points of sodium and lithium metasilicates, we could investigate both crystalline phases throughout the temperature ranges where dynamical changes were suggested to occur. Both ^{23}Na and ^{7}Li can be investigated readily by high-temperature NMR on normal materials, but studies of ^{29}Si static spectra at high temperature generally require isotopic enrichment. As previous measurements did not point to significant silicate chain dynamics in Li_2SiO_3, ^{29}Si NMR spectra were recorded for Na_2SiO_3 only.

Experimental methods

The crystalline Li_2SiO_3 was previously studied (Téqui et al. 1992; Richet et al. 1996). Its purity was confirmed by ^{29}Si MAS NMR, with a single, narrow peak at −74.7 ppm. Several new samples of crystalline Na_2SiO_3 were synthesized. All were prepared in the same fashion from reagent grade Na_2CO_3 and 95% enriched $^{29}SiO_2$ or natural SiO_2 in final sample amounts of about 0.5 and 100 g for the isotopically enriched and natural samples, respectively. About 0.2 wt% CoO was added to speed ^{29}Si spin-lattice relaxation. This concentration was low enough so that whether or not all of the Co remained in solid solution in the Na_2SiO_3 product, it could cause only an insignificant amount of partial melting, regardless of its valence state. The mixtures were ground in an agate mortar and then heated in platinum crucibles, decarbonated overnight near 750 °C, melted for about 1 h at 1300 °C, and eventually held overnight at 800 °C to achieve complete crystallization. Hygroscopic Na_2SiO_3 was stored in a dessicator under vacuum and containing P_2O_5 drying agent and was crushed and loaded into the sample containers in a glove box filled with dry N_2. All Na_2SiO_3 samples were characterized by ^{29}Si MAS NMR before and after high-temperature NMR.

The first samples were loaded into capsules made of hexagonal boron nitride and were studied under a N_2-5%H_2 atmosphere in the high-temperature NMR experiments. No evidence of reaction of Li_2SiO_3 with the capsule material was found up to the highest temperatures investigated. In contrast, ^{29}Si NMR experiments on Na_2SiO_3 indicated the formation of a sodium borosilicate liquid phase above about 900 °C through the appearance of a narrow, liquid-like ^{29}Si peak near −83 ppm, and the development of a film of glassy material at the contact between sample and container. On such samples after cooling, ^{11}B and ^{29}Si MAS NMR showed the presence of a minor amount of a borosilicate glass phase. To prevent such a reaction, we then used samples that had been cast in 10 mm inside diameter graphite or 5 mm platinum tubes, which were placed directly within the Mo rf (radio frequency) coil without a sample container for the NMR experiments. Under these conditions, melting was nevertheless observed to begin at temperatures about 100° below the congruent melting temperature. Heating experiments made under various conditions (including samples with and without Co doping) showed that this was related to the N_2-5%H_2 gas flow, probably through compositional changes caused by reduction and volatilization of Na. Under air, in contrast, the Na_2SiO_3 samples could be heated up to the immediate vicinity of the melting point without evidence for partial melting. Later experiments were thus done with ''containerless'' samples, in contact only with a platinum rf coil, after the probe was modified to run in air (Sen and Stebbins 1997).

NMR data were collected with a modified Varian VXR-400S spectrometer at 105.8 MHz for ^{23}Na, 130.4 MHz for ^{7}Li, 58.6 MHz for ^{6}Li, and 79.5 MHz for ^{29}Si. The high temperature (T) data (all on ''static,'' non-spinning samples) were collected with a home-built probe (Stebbins 1991). Temperatures inside the probe were calibrated in separate experiments where a thermocouple was mounted in the sample container in the same way as for the actual experiments. The uncertainty of temperatures determined from these calibrations is ±10 °C. The spectra were obtained with short pulses (<20° rf tip angle) and delay times of 1 s for ^{23}Na and ^{7}Li. The ^{29}Si and ^{6}Li spectra were acquired with delay times ranging from 1 s to 1 h. No differential relaxation was observed in experiments with varying delays between pulses. Spin-lattice relaxation time (T_1) measurements were made using a saturation-recovery pulse sequence. Spin echo spectra ($90° - \tau - 180°$ pulse sequence) were also acquired to examine the effects of instrumental deadtime on the shapes of the relatively broad ^{29}Si spectra.

For the room-temperature MAS experiments, we used either a Varian probe with a spinning speed of 7 kHz or a Doty Scientific MAS probe with a spinning speed of 11 kHz. Peak positions in all spectra were referenced to an external 1M NaCl solution (^{23}Na), saturated LiCl solution (^{7}Li, ^{6}Li), or tetramethylsilane (^{29}Si) at room temperature and are reported as relative frequency in parts per million (ppm). As Na_2SiO_3 crystals break apart into needle-shaped fragments when crushed, the final MAS sample of this phase was mixed with epoxy before being ground to avoid preferred orientation resulting from anisotropic particle shape. The undistorted MAS quadrupolar line shape obtained in this way was quite different from spectra collected on the pure, crushed sample.

Results

^{7}Li in lithium metasilicate

Static ^{7}Li spectra of Li_2SiO_3 (Fig. 1) have well-defined quadrupolar powder patterns at all temperatures, indicating that Li is not mobile enough to have a completely averaged, isotropic environment, even at 50° below the melting point. The spectra recorded between room tem-

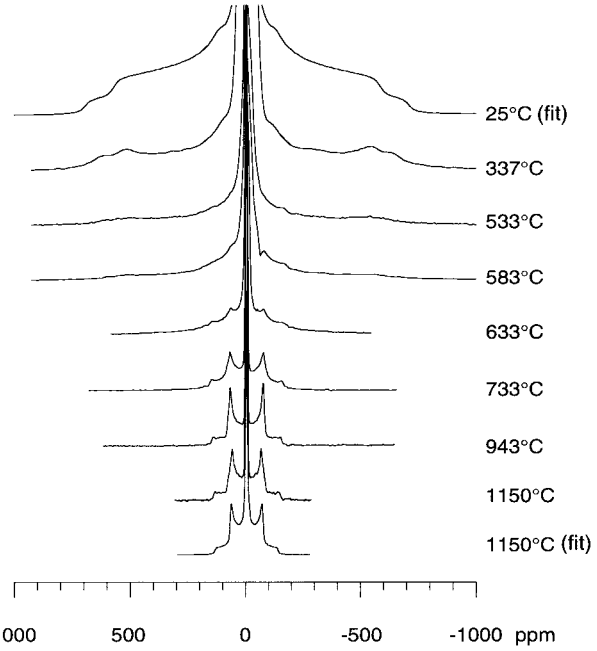

FIGURE 1. Static ^{7}Li spectra of Li_2SiO_3, with selected simulations. Spectra show all three quadrupolar transitions, including central, 1/2 to −1/2, and ''satellite,'' ±1/2 to ±3/2. The intensities of the 337 °C spectrum are somewhat distorted relative to the fit, possibly because of instrumental deadtime, but the location of the inflections (singularities) accurately define the fit parameters as given in the text. The small dip to the right of the main peak in the 583 °C spectrum is an artifact.

perature and about 340 °C can be fitted with a quadrupolar coupling constant (QCC) of 0.15 MHz and a quadrupolar asymmetry parameter (η) of 0.65. Point charge calculations done with the crystal structure data (Völlenkle 1981) and the program ''ptchg'' (Spearing 1994) predict $\eta = 0.61$, close to the experimental value, but a QCC of 0.45 MHz, which is about three times larger than the experimental result. At higher *T*, the high frequency ''wings'' of the spectra, due to the ±1/2 to ±3/2 transitions, become less distinct. Above about 600 °C a second, much narrower quadrupolar powder pattern emerges, which can be accurately fitted with QCC = 0.03 MHz and $\eta = 0$.

^{6}Li in lithium metasilicate

The ^{6}Li MAS spectrum of Li_2SiO_3 contained a single narrow peak (<0.3 ppm) centered at 0.44 ppm, in the center of the range for tetrahedral Li sites determined from other silicates (Xu and Stebbins 1995a). As has been often observed for this nuclide, T_1 was very long, on the order of hundreds of seconds.

^{23}Na in sodium metasilicate

The room-temperature ^{23}Na MAS spectrum for Na_2SiO_3 exhibits a quadrupolar peak shape for the central transition that can be fitted with QCC = 1.4 MHz and η = 0.8. These values are comparable to the values predicted from ptchg and the crystal structure data (McDonald and Cruickshank 1967) of QCC = 1.1 MHz and $\eta = 0.88$.

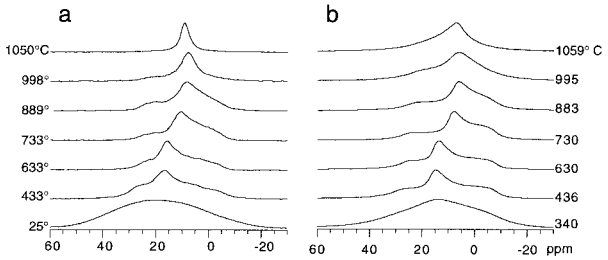

FIGURE 2. Static ^{23}Na spectra of Na_2SiO_3 measured (**a**) in N_2-5%H_2; and (**b**) in air without container. Only the central, 1/2 to −1/2 transition is observed.

Figure 2 shows the static spectra from 430 to 1050 °C (only 39 °C below the melting point) for experiments made under the reducing atmosphere with a BN sample container and under air with a containerless sample. Preferred orientation was less of a problem in the former series because the sample was made up of many small fragments of material in random orientations, but the spectra were affected by early melting at the highest temperatures, apparently caused by compositional change (see experimental section). This problem was avoided in the latter series of experiments done in air, but then spectra were somewhat distorted, as the cast Na_2SiO_3 cylinders were made up of crystals that had some preferred, radial orientation.

As in the ^{23}Na MAS experiments, only the central, 1/2 to −1/2 transition was observed in the static spectra, as is typical for this nuclide because of its large quadrupolar moment. The static spectrum at room temperature is broadened to the point of being featureless, but begins to be better resolved by 430 °C, probably because Na^+ motion is rapid enough at this temperature to average out Na-Na dipolar couplings and eliminate this broadening mechanism. Above this temperature, the peak shape can best be fitted with a sum of two quadrupolar patterns (Fig. 3 and Table 1). The use of two peaks in the fitting procedure is further justified by the difference in peak shapes observed when different pulse lengths were used: two peaks with different 180° times (the pulse length needed to invert the magnetization and thus null the spectrum) can clearly be seen from 430 to 1000° C (Fig. 4). One of these sites (site 1) is consistent with that indicated by both crystal-structure determinations and the MAS spectrum at room temperature; the other (site 2) has a larger QCC and an isotropic chemical shift at higher frequency. In addition, both peak positions noticeably shift to lower frequency by about 5 to 6 ppm between 633 and 733 °C, i.e., in the range of the previously observed phase transition (Richet et al. 1996). The centers of mass of the peaks shift to a slightly lower frequency by an amount consistent with thermal expansion (George and Stebbins

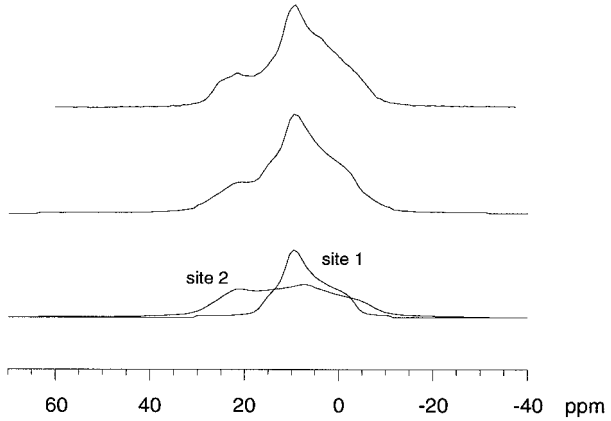

FIGURE 3. ^{23}Na peak shape in Na_2SiO_3 in N_2-5%H_2 at 783 °C. Top = experimental spectrum; middle = fitted spectrum; bottom = the two components used in the simulation. To facilitate fitting, the two peaks were separated by subtracting spectra obtained using different pulse lengths (as in Fig. 4).

1995) at temperatures above and below the phase transition.

At high temperatures (above 900 °C), spectra recorded under both kinds of atmosphere become narrower. In N_2-5%H_2 gas, the peak collapses completely to a narrow Lorentzian line at 14 ppm. The sample after this run was not extensively melted, as might be suggested by the narrow peak; rather, there was a thin layer of sintered crust on the outside, with unaltered, crystalline powder on the inside. The sample run in air showed no sign of melting, either in the ^{29}Si spectra (see below) or from microscopic examination after the experiment. For this sample, the ^{23}Na peak also showed narrowing near the melting point, but not as extensively as observed for experiments in the reducing atmosphere.

The ^{23}Na spin-lattice relaxation times are plotted in Figure 5 as a function of temperature. In some cases, especially near the changes in slope, fitting the results of the saturation-recovery experiment with a single relaxation time only approximates the observed behavior, which could be more accurately fitted with a sum of two exponentials with two time constants. The results of this procedure, are, however, useful for qualitative comparisons. Relaxation times show a pattern typical for minerals

TABLE 1. Fit parameters for static ^{23}Na spectra of Na_2SiO_3

	Site 1			Site 2		
T (°C) ±10	δ_{iso} ppm, ±2	QCC MHz, ±0.1	η ±0.1	δ_{iso} ppm, ±2	QCC MHz, ±0.1	η ±0.1
433	19	1.3	1	25	1.4	0.6
533	19	1.2	1	25	1.2	0.6
633	18	1.1	1			
733	13	1.0	0.9	19	1.5	0.5
783	12	1.0	0.9	18	1.5	0.5
835	11	1.0	0.9	19	1.4	0.4
889	11	1.0	0.9	19	1.3	0.4

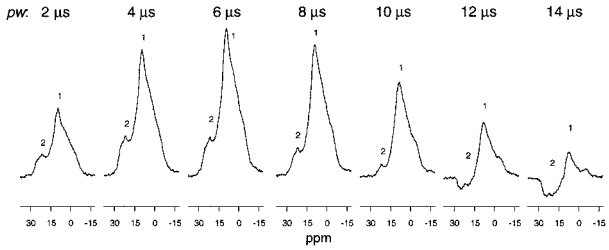

FIGURE 4. ^{23}Na spectra of Na_2SiO_3 at 783° C obtained using different pulse rf widths *pw*. Seven spectra are shown, with scales in ppm. Two sites with different 180° (inversion) times can be seen, as also shown in Figure 3; peak 2 is nulled and inverted at slightly shorter pulse lengths than peak 1.

(Spearing et al. 1994; George and Stebbins 1995), decreasing first slowly with temperature, and then more steeply above about 350 °C (i.e., $1000/T = 1.6$). This decrease has commonly been attributed to a change in the relaxation mechanism, probably from a predominantly paramagnetic mechanism to a quadrupolar mechanism controlled by enhanced Na^+ motion. In addition, however, Na_2SiO_3 displays an apparent T_1 minimum at 1000–1050 °C (i.e., $1000/T = 0.76$) that is seen in both data sets, above which T_1 begins to increase again. This ''minimum'' occurs at a value of $T_1 = 0.0008$ s. The relaxation times are also affected by the atmosphere under which the measurements are made; relaxation times are shorter at high temperature in air than in the reducing conditions. Without extensive further studies we cannot be certain that the effects of paramagnetic centers, or changes in such effects caused by variation in their valence, are completely negligible at high T.

^{29}Si in Na_2SiO_3

The ^{29}Si MAS NMR spectrum at room temperature (collected for all samples, both enriched and isotopically

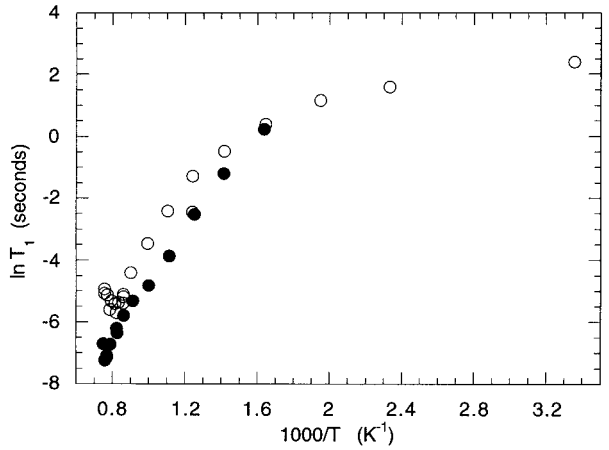

FIGURE 5. ^{23}Na spin-lattice relaxation times (T_1) in Na_2SiO_3. Open circles are data from experiment in N_2-5%H_2; closed circles are from the experiment in air. The natural logarithm of T_1 is plotted vs. the inverse of absolute temperature in K. Uncertainties are 1 to 1.5 times the size of the symbols.

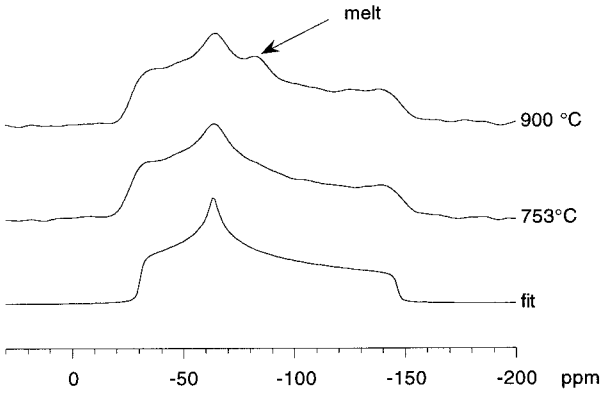

FIGURE 6. Static ^{29}Si spectrum of Na_2SiO_3 at 753 °C (bottom) and 900 °C (top) under N_2-5%H_2, showing the appearance of a narrow melt peak near −82 ppm.

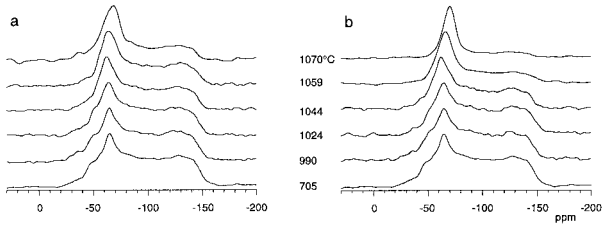

FIGURE 7. ^{29}Si spectra of Na_2SiO_3 in air without container. (**a**) one-pulse spectra; (**b**) spin-echo spectra. The line shape is somewhat distorted relative to those run in N_2-5%H_2, due to preferred orientation of the crystals in the cast cylindrical sample.

normal) showed the single site expected for Na_2SiO_3 and no evidence for any other crystalline phases. The narrow peak has an isotropic chemical shift (δ_{iso}) of −76.8 ppm. From room temperature to about 70 or 80 °C below the melting point, the static high-temperature Si spectra display a typical chemical shift anisotropy (CSA) pattern (e.g., Fig. 6, middle spectrum) (Kirkpatrick 1988; Stebbins 1988). The 753 °C spectrum (the best resolved) was fitted with the CSA tensor parameters $\delta_{11} = -26$, $\delta_{22} = -62$, and $\delta_{33} = -152$ ppm ($\delta_{iso} \approx -79.6$), similar to previous data collected at ambient temperature and typical of the biaxial symmetry seen for all known Q^2 sites in chain silicates (Stebbins 1995b). (Q^n refers to an Si site with *n* bridging O links to other tetrahedral cations such as Si or Al.) In the spectra obtained under N_2-5%H_2 gas, a narrow, symmetrical peak typical of a molten phase appears at about 900 °C (Fig. 6). It increases in intensity with time and temperature. This melt peak is not present for the sample heated in air (Fig. 7). However, significant changes do occur in these spectra between 1044–1070 °C. The high frequency (less negative ppm) shoulder, which is characteristic of the biaxial symmetry for Q^2 sites in chain silicates, disappears as the peak maximum moves in this direction, resulting in what appears to be a uniaxial powder pattern. In addition, the intensity in the low frequency (more negative ppm) part of the spectrum is anomalously low in the spin echo spectra, which at lower temperature are nearly identical to the 1-pulse spectra.

DISCUSSION

Lithium metasilicate

If the static ^7Li spectrum for Li_2SiO_3 at ambient temperature is compared directly to those collected above 700 °C (Fig. 1), an obvious interpretation would be that the static geometry of the Li^+ site changes over this interval from a biaxially distorted tetrahedral environment to a uniaxial, more nearly perfect tetrahedral environment with a much lower electric field gradient and thus QCC. However, the progressive change in peak shape between about 300 and 750 °C does not support this conclusion, as the high and low frequency ''wings'' of the spectra (the ±1/2 to ±3/2 transitions) first broaden to the point of being almost unobservable, then grow back in at the positions appropriate to the high *T*, reduced QCC and η values. In contrast, a progressive change in the static shape of the site would result in a gradual movement of these features toward the center of the spectrum without changes in shape and definition. Neither a major, progressive change in static structure, nor an abrupt phase transition, is observed in high temperature X-ray diffraction (XRD) data (Richet et al. 1996). A likely explanation of the NMR data is thus a partial dynamical averaging of the spectra caused by Li^+ exchange from one position to another. Complete, ''liquid-like'' motional averaging, where in the spectrum collapses to a single, narrow peak, is clearly not observed, however. This requires that the Li motion responsible for the averaging does not sample a wide enough set of site geometries and orientations for their time average to achieve spherical symmetry. The latter phenomenon is typical of Li^+ and Na^+ motion in glasses (Stebbins 1995a; George and Stebbins 1996), but apparently is not allowed by the constrained, long-range order of this crystal lattice.

A rigorous treatment of these results is difficult, in part because even at ambient temperature, motional averaging either within or among Li sites may already affect the ^7Li spectra, resulting in the observation of a QCC value lower than that predicted from the X-ray structure. Furthermore, the orientation of the electric field gradient (efg) tensor with respect to the crystallographic axes cannot be determined without single-crystal NMR data. However, the change in the peak shape at $T > 300$ °C does reveal useful information about Li^+ dynamics. Although the structure contains only one crystallographic Li site, with respect to the external magnetic field there are multiple (at most four), symmetry-related orientations of this distorted LiO_4 tetrahedron within any single crystallite in a powdered sample. If hopping of Li^+ cations between adjacent sites occurs at a frequency that is large compared to the total spectral width at ambient temperature (about 195 kHz), a time average of the spectra for the differently oriented sites will be observed in the spectrum. This average must have a lower mean QCC, and the asymmetry parameter η will be reduced to zero if the static efg tensor axes are related by crystal symmetry.

An approximate idea of the frequency of Li^+ site hopping can be obtained from the observation that in motional averaging, the fully averaged spectrum appears when the exchange frequency is several times the frequency separation of the features being averaged (Stebbins 1995a), in this case the extreme high and low frequency ''wings'' of the $\pm 1/2$ to $\pm 3/2$ low temperature powder pattern. Taking the 733 °C spectrum as nearly fully averaged, we would expect the hopping frequency to be 5 to 10 times 195 kHz, i.e., on the order of 1 to 2 Mhz. To compare with Li mobility in previously studied Li-ion conductors at lower temperature, we can extrapolate with a typical Arrhenian activation energy of 80 kJ/mol (Shannon et al. 1977). Using a standard model to relate site hopping to ionic conductivity (assuming 3-D conduction and a mean jump distance of 0.29 nm, as in the room temperature structure), we estimate the conductivity at 227 °C to be of the order of 2×10^{-7} $(\Omega m)^{-1}$ (Stebbins et al. 1995; Xu and Stebbins 1995b). Such a conductivity would be fully three orders of magnitude below that of stoichiometric Li_4SiO_4 and six orders of magnitude below that of the Al-doped solid solution of that phase (Shannon et al. 1977). Thus, although we can clearly see the effects of Li site hopping at high temperature in Li_2SiO_3, it is a much poorer ionic conductor than other Li-silicates.

Sodium metasilicate: ^{23}Na

The Na spectra also show several changes with temperature. The large shift in peak position and shape between about 633 and 733 °C can be attributed to the phase transition observed near this temperature in XRD data (Richet et al. 1996). The observed change in the peak maximum or the derived isotropic chemical shift of site 1 (Fig. 3) is consistent with an increase in average bond length of the site by 0.01 nm or a change in the coordination number from 5 to 6 or 7 (Xue and Stebbins 1993; George et al. 1997). Site 2, most clearly detected by its nulling and inversion at a slightly shorter 180° pulse than site 1 (Fig. 4), may be smaller than site 1, because its fitted chemical shift is at higher frequency. This site may be tetrahedral, as is the Li site in Li_2SiO_3: The largest axis of thermal expansion in Na_2SiO_3 is along the *c* axis, and one of the O atoms in the NaO_5 trigonal bipyramid might be stretched out too far from the Na to be part of its coordination sphere as the material is heated. Point charge calculations predict a QCC of about 1 MHz and η around 0.6 for this kind of site, similar to observations (QCC = 1.4, η = 0.55). However, this solution is only one of several different possibilities for the site splitting.

At higher temperature, the spectra (Fig. 2) change further in the form of a gradual narrowing toward a featureless Lorentzian peak shape, indicative of motional narrowing. Unlike Li in Li_2SiO_3, the peak becomes significantly narrowed just below the melting temperature, suggesting rapid, isotropic motion among many sites with a wide range of orientations and/or electric field gradients, before the material is fully melted. This liquid-like peak is present even though the sample after recovery clearly did not undergo extensive bulk melting. This motional narrowing begins to become apparent in the calorimetric premelting range.

The sample run under the N_2-5%H_2 atmosphere exhibited an even larger degree of motional narrowing. This implies that Na is more mobile under reducing conditions, possibly because Na loss or H addition creates defects that promote diffusion.

The apparent minimum in the T_1 curve could result from a single spin-lattice relaxation mechanism, in which case it would mark the point of the maximum spectral density of Na^+ hopping frequencies at the Larmor frequency of 105.8 MHz (Stebbins 1995a). The T_1 value at this minimum is about eight times higher than that typically observed in silicate liquids (~0.0001 s) (Liu et al. 1987; George and Stebbins 1996). This difference could be explained in part by the smaller QCC values observed in the crystal (1 to 1.5 MHz vs. 2.5 to 3 in the liquid), as T_1 is expected to scale with $(1/QCC)^2$ (George and Stebbins 1996). However, the difference between the results obtained for the two gas atmospheres would be difficult to understand, as the depth of the T_1 minimum should be a function of the structure only, for a given relaxation mechanism.

It is thus more likely that the observed T_1 ''minimum'' for Na_2SiO_3 results from a relatively abrupt change in the Na^+ dynamics that shifts the average hopping frequency to much greater values over a narrow temperature range. The appearance of this transition at a lower temperature and a higher T_1 value for the sample run in a reducing atmosphere is consistent with an increased Na^+ mobility in this sample, although the explanation of the T_1 differences at lower temperatures remains unclear. This phenomenon has been implicated to explain discontinuities in T_1 curves at displacive phase transitions in cristobalite (SiO_2) and cryolite (Na_3AlF_6) (Spearing et al. 1992; Spearing et al. 1994), and it was in those cases associated with the dynamical character of the high-temperature, high-symmetry structures.

Sodium metasilicate: ^{29}Si

The changes in the ^{29}Si spectra of Na_2SiO_3 near the melting point are somewhat subtle but are clearly significant. First of all, the lack of any liquid-like features (e.g., a narrow, Lorentzian peak) in the sample run in air demonstrates that well within the calorimetric premelting range, no actual melting occurs to form a distinct liquid phase, with a detection limit of a few percent. Thus, as has been indicated in previous studies, the large premelting heat capacity anomaly in Na_2SiO_3, and the major changes that occur in its Raman spectrum in this temperature range, are inherent to the structure and dynamics of the crystalline phase itself.

The ^{29}Si spectra also show no evidence of the development of a significant population of Q^4 sites in the premelting range (at a detection level of about 2%), as might be expected if significant Si-O bond breaking and rear-

rangement were taking place in a melt-like fashion. However, partial motional averaging of the spectrum does begin to be visible at about 1000 °C. The static, low-temperature peak shape is typical of Q^2 sites in chain silicates, which have chemical shift anisotropies that are inherently biaxial because such sites have no topologically unique axis of cylindrical symmetry. The high-temperature peak shape for Na_2SiO_3 resembles that for Q^3 sites in silicates, which do have an inherent symmetry axis marked by the bond between the Si and the single non-bridging oxygen (NBO). Stoichiometry, of course, does not allow the Q^2 sites in Na_2SiO_3 to actually be converted to Q^3 sites. Instead, we suggest that some type of librational motion of the SiO_4 tetrahedra becomes important in the premelting range, producing partial averaging of the spectrum. Partial rotation about the bonds between Si and the bridging O atoms, such that the two NBO positions become averaged, is an example of a motion that could possibly result in the observed spectral changes, but a detailed explanation requires a single-crystal NMR study that links the chemical shift anisotropy tensor to the crystal structure. A dynamical explanation of the observed changes in the ^{29}Si spectra is supported by the similarities (at low temperature) and differences (at high temperature) between the 1-pulse and spin-echo spectra (Fig. 7). In the latter, after an initial 90° preparation pulse, a 180° refocusing pulse is given after a delay τ. If, during this delay, some exchange occurs, part of the magnetization will not re-focus into the spin echo that is subsequently Fourier transformed to yield the spectrum. This may explain the anomalously low intensities in the low frequency (more negative ppm) parts of the high *T* spin echo spectra when compared to the 1-pulse data. In any case, the severe deformation of the Si-O bonds that is likely to accompany extreme librational motion may be responsible for the large changes that occur in the high frequency region of the Raman spectra in the premelting regime (Richet et al. 1996).

Dynamical contrast between Li_2SiO_3 and Na_2SiO_3

Li^+ cation mobility is high in many classes of silicate, oxide, and other materials, apparently because its relatively small size allows motion from one cation site to another with relatively minor energetic consequences (Shannon et al. 1977; Stebbins et al. 1995; Xu and Stebbins 1995b). Although Li_2SiO_3 does not appear to be a particularly good ionic conductor, it is still likely that the local mechanism of Li^+ site exchange is similar to that in better-studied silicates, where rapid Li^+ diffusion can occur without a major contribution to the heat capacity and without major perturbation of the silicate or oxide network. In Li_2SiO_3, our ^7Li NMR data are consistent with Li^+ site hopping among a few ordered Li sites without any disordering of Si or O positions, as expected in such decoupled motion.

In contrast, Na^+ motion near the melting point of Na_2SiO_3 appears to be more ''liquid-like'' in the sense of sampling many differently oriented sites. This may take place if diffusion of the larger Na^+ cation requires that it hop into normally unoccupied sites in the structure, or if the Na^+ sites are fluctuating in shape and size because of SiO_4 tetrahedral librations. In either case, relatively large energetic consequences may be expected, which would result in the observed heat capacity anomaly. Silicate chain motion and Na^+ diffusion are likely to be coupled, as tetrahedral motion may open ''windows'' between O atoms that allow Na^+ to jump from one site to another more easily. A related mechanism has been suggested for the coupling of Na^+ site hopping and librations of AlO_6 octahedra in cryolite (Spearing et al. 1994).

In conclusion, these NMR results are not only consistent with the information drawn from XRD and Raman spectroscopy (Richet et al. 1984; Richet et al. 1996), but give a more detailed picture of alkali cation diffusive motion and dynamics of the silicate framework. Single-crystal NMR studies could lead to more specific information about the mutual relationships of these phenomena. The relatively small enthalpy cost of such Na^+ and Li^+ diffusive motion in the solid state, points to most of the enthalpy of melting being probably associated with disruption of the silicate framework. Likewise, the so-called configurational heat capacity of liquids should correspond primarily to further changes affecting the silicate entities.

Acknowledgments

This work was supported by NSF grant EAR-9506393 to J. Stebbins. We gratefully acknowledge the support of P. Richet while at the Stanford School of Earth Sciences as an Alan Cox Visiting Professor.

References cited

Farnan, I. and Stebbins, J.F. (1994) The nature of the glass transition in a silica-rich oxide melt. Science, 265, 1206–1209.

George, A.M. and Stebbins, J.F. (1995) High-temperature ^{23}Na MAS NMR data for albite: Comparison to chemical-shift models. American Mineralogist, 80, 878–884.

——— (1996) Dynamics of Na in sodium aluminosilicate glasses and liquids. Physics and Chemistry of Minerals, 23, 526–534.

George, A.M., Sen, S., and Stebbins, J.F. (1997) ^{23}Na chemical shifts and local structure in crystalline and glassy sodium borates and germanates. Solid State Nuclear Magnetic Resonance, 10, 9–18.

Hesse, K.F. (1977) Refinement of the crystal structure of lithium polysilicate. Acta Crystallographica, B33, 901–902.

Kirkpatrick, R.J. (1988) MAS NMR spectroscopy of minerals and glasses. In Mineralogical Society of America Reviews in Mineralogy, 18, 341–403.

Kracek, F.C. (1930) The system sodium oxide-silica. Journal of Physical Chemistry, 34, 1583–1598.

Liu, S.B., Pines, A., Brandriss, M., and Stebbins, J.F. (1987) Relaxation mechanisms and effects of motion in albite ($NaAlSi_3O_8$) liquid and glass: a high temperature NMR study. Physics and Chemistry of Minerals, 15, 155–162.

McDonald, W.S. and Cruickshank, D.W.J. (1967) A reinvestigation of the structure of sodium metasilicate. Acta Crystallographica, 22, 37–43.

Naylor, B.F. (1945) High-temperature heat contents of sodium metasilicate and sodium disilicate. Journal of the American Chemical Society, 67, 466–467.

Phillips, B.L., Thompson, J.G., Xiao, Y., and Kirkpatrick, R.J. (1993) Constraints on the structure and dynamics of the beta-cristobalite polymorphs of SiO_2 and $AlPO_4$ from ^{31}P, ^{27}Al and ^{29}Si NMR spectroscopy to 770 K. Physics and Chemistry of Minerals, 20, 341–352.

Richet, P. and Fiquet, G. (1991) High-temperature heat capacity and pre-

melting of minerals in the system MgO-CaO-Al_2O_3-SiO_2. Journal of Geophysical Research, 96, 445–456.

Richet, P., Bottinga, Y., and Téqui, C. (1984) Heat capacity of sodium silicate liquids. Journal of the American Ceramic Society, 67, C7–C8.

Richet, P., Ingrin, J., Mysen, B.O., Courtial, P., and Gillet, P. (1994) Premelting effects in minerals; an experimental study. Earth and Planetary Science Letters, 121, 589–600.

Richet, P., Mysen, B.O., and Andrault, D. (1996) Melting and premelting of silicates; Raman spectroscopy and X-ray diffraction of Li_2SiO_3 and Na_2SiO_3. Physics and Chemistry of Minerals, 157–172.

Rigamonti, A. (1984) NMR-NQR studies of structural phase transitions. Advances in Physics, 33, 115–191.

Sen, S. and Stebbins, J.F. (1997) Na ion transport in borate and germanate glasses and liquids: a ^{23}Na and ^{11}B NMR spin-lattice relaxation study. Physical Review B, 55, 3512–3519.

Shannon, R.D., Taylor, B.E., English, A.D., and Berzins, T. (1977) New Li solid electrolytes. Electrochimica Acta, 77, 783–796.

Spearing, D.R. (1994) ptchg: a FORTRAN program for point-charge calculations of electric field gradients (EFGs). Computers and Geosciences, 20, 615–624.

Spearing, D.R., Farnan, I., and Stebbins, J.F. (1992) Dynamics of the a-b phase transitions in quartz and cristobalite as observed by in-situ high temperature ^{29}Si and ^{17}O NMR. Physics and Chemistry of Minerals, 19, 307–321.

Spearing, D.R., Stebbins, J.F., and Farnan, I. (1994) Diffusion and the dynamics of displacive phase transitions in cryolite (Na_3AlF_6) and chiolite ($Na_5Al_3F_{14}$): multi-nuclear NMR studies. Physics and Chemistry of Minerals, 21, 373–386.

Stebbins, J.F. (1988) NMR spectroscopy and dynamic processes in mineralogy and geochemistry. In Mineralogical Society of America Reviews in Mineralogy, 18, 405–430.

———(1991) Nuclear magnetic resonance at high temperature. Chemical Reviews, 91, 1353–1373.

———(1995a) Dynamics and structure of silicate and oxide melts: nuclear magnetic resonance studies. In Mineralogical Society of America Reviews in Mineralogy, 32, 191–246.

———(1995b) Nuclear magnetic resonance spectroscopy of silicates and oxides in geochemistry and geophysics. In T.J. Ahrens, Ed., Handbook of Physical Constants, p. 303–332. American Geophysical Union, Washington, D.C.

Stebbins, J.F., Carmichael, I.S.E., and Moret, L.K. (1984) Heat capacities and entropies of silicate liquids and glasses. Contributions to Mineralogy and Petrology, 86, 131–148.

Stebbins, J.F., Farnan, I., Williams, E.H., and Roux, J. (1989) Magic angle spinning NMR observation of sodium site exchange in nepheline at 500° C. Physics and Chemistry of Minerals, 16, 763–766.

Stebbins, J.F., Xu, Z., and Vollath, D. (1995) Cation exchange rate and mobility in aluminum-doped lithium orthosilicate: high-resolution lithium-6 NMR results. Solid State Ionics, 78, L1–L8.

Téqui, C., Grinspan, P., and Richet, P. (1992) Thermodynamic properties of alkali silicates: heat capacity of Li_2SiO_3 and lithium-bearing melts. Journal of the American Ceramic Society, 75, 2601–2604.

Ubbelohde, A.R. (1978) The Molten State of Matter, 454 p. Wiley, New York.

Völlenkle, H. (1981) Verfeinerung der Kristallstrukturen von Li_2SiO_3 und Li_2GeO_3. Zeitschrift für Kristallographie, 154, 77–81.

Xu, Z. and Stebbins, J.F. (1995a) ^{6}Li and ^{7}Li NMR chemical shifts, relaxation, and coordination in silicates. Solid State Nuclear Magnetic Resonance, 5, 103–112.

———(1995b) Cation dynamics and diffusion in lithium orthosilicate: two-dimensional lithium-6 NMR. Science, 270, 1332–1334.

Xue, X. and Stebbins, J.F. (1993) ^{23}Na NMR chemical shifts and the local Na coordination environments in silicate crystals, melts, and glasses. Physics and Chemistry of Minerals, 20, 297–307.

Manuscript received February 23, 1998
Manuscript accepted March 4, 1998
Paper handled by Hans Keppler